Structural and dielectric properties of synthetic glycolipids in mixtures with water

Reiner Zorn,* Michael Grünert,‡ Oswald Lockhoff,§ and Günter Nimtz‡

*Forschungszentrum Jülich, Institut für Festkörperforschung, D-5170 Jülich 1; ‡II. Physikalisches Institut, Universität zu Köln, D-5000 Köln 41; and §Bayer AG, Geschäftsbereich Pharma, D-5600 Wuppertal, Federal Republic of Germany

ABSTRACT Three synthetically produced glycolipids, *N*-(β-D-glucopyranosyl)-*N*-octadecyl-stearoylamide (OSGA), *N*-(β-D-glucopyranosyl-*N*-octadecyl-oleoylamide (OOGA), *N*-(β-D-galactopyranosyl)-*N*-octadecyl-lauroylamide (OLGA) have been studied in different mixtures with water by x-ray diffraction and dielectric measurements with microwaves at 9.4 GHz. The measurements were performed in the temperature range −50–70°C. X-Ray diffraction revealed a direct $L_{\beta'} \rightarrow H_{II}$ transition at 20°C, 60°C, and 45°C depending on the glycolipid species but nearly not on the water content. The hexagonal phases are saturated at a water content of ≈20 wt%. The lamellar phase absorbs even less water (<10 wt%). The dielectric data show that in the H_{II} phase the binding of water is stronger than in the $L_{\beta'}$ phase. In the temperature range below 0°C, OSGA and OOGA show a "subzero transition" due to the freeze-out of water in a separate ice phase. This transition can be seen in an abrupt decrease of the dielectric function because the dielectric response of ice is much smaller at microwave frequencies. OLGA does not show the subzero transition but an additional transition, hexagonal → distorted hexagonal at 60°C.

INTRODUCTION

The first investigations of physical properties of biological model membranes were carried out on phospholipids, which have easily been obtained by synthesis for more than 35 years. Recently, glycolipids, which are known to play important roles in biological systems (1), have entered the scope of research (for a summary see reference 2). In most investigations lipid extracts from natural biological membranes have been examined. Those are usually mixtures in which the polar headgroups are identical, but the chains represent a natural set of different fatty acids.

In this paper we present a study on synthetic glycolipids of single species, which are not found in nature. Nevertheless they were shown to have an interesting biological profile reflecting immunomodulating properties, i.e., the stimulation of antibody production in vitro (3). From those chemically pure materials a well-defined phase behavior, i.e., sharp phase transitions can be expected. The methods we used were the classical technique of x-ray diffraction to explore the structural properties and the measurement of the dielectric function at microwave frequencies that we had applied on phospholipid systems (4) and microemulsions (5).

MATERIALS AND METHODS

The glycolipids we used in our investigations are synthetically modified analogues of naturally occurring glycosphingosides. They can easily be obtained in two steps by reacting glucose with an *N*-alkylamine, and acylating the resulting β-D-glucosylamine with fatty acid derivatives to yield *N*-alkyl-*N*-(β-D-glucopyranosyl)-carboxamides (patent EP 091 645 [1987/1983]; Bayer AG, Wuppertal, FRG). Three species were synthesized (Fig. 1): *N*-(β-D-glucopyranosyl)-*N*-octadecyl-stearoylamide (OSGA);[1] *N*-(β-D-glucopyranosyl)-*N*-octadecyl-oleoylamide (OOGA); *N*-(β-D-galactopyranosyl)-*N*-octadecyl-lauroylamide (OLGA). The first two, OSGA and OOGA, differ only in one double bond in one of the hydrocarbon chains. OLGA has two chains of unequal length; besides, its headgroup contains galactose instead of glucose.

The lipids were mixed with ultra-high quality water ($\rho \approx 18$ MΩ cm) from an ELGASTAT water conditioner (Elga Ltd., High Wycomb Bucks, UK). Mixtures were set to ~0, 5, 10, 20, and 30 wt% water because previous experiments showed that larger water contents would produce no further changes in the phase behavior (saturation).

The mixtures were tempered for ~48 h at a temperature significantly above the main phase transition before filling. For the dielectric measurements, the final water content of the mixed samples was controlled after the measurement by the Karl-Fischer method (moisture meter CA-02, Mitsubishi, Tokyo, Japan). In the case of the x-ray samples their quantities were not large enough (≈10 mg only) to get reliable values this way; so the water content of the "dry" glycolipids was measured with the moisture meter and deduced from the calculated amount of water to be added in preparation. Clearly, this procedure is not as exact, resulting in an error of ~1 wt%.

The x-ray measurements were mostly carried out on a Kratky-type small-angle camera (A. Paar GmbH, Graz, Austria) using Ni-filtered Cu-K_α radiation ($\lambda = 1.542$ Å). As an x-ray source a 1.4 kW fixed-anode tube was used (Siemens AG, Karlsruhe, FRG). The diffracted x-rays were registered by a movable scintillation detector, the registration time for a whole diffractogram was ~20 min. The camera works

[1] *Abbreviations used in this paper:* DAPE, L-α-diarachidoyl-phosphatidylethanolamine; DMPC, L-α-dimyristoyl-phosphatidylcholine; DPPC, L-α-dipalmitoyl-phosphatidylcholine; OLGA, *N*-(β-D-galactopyranosyl)-*N*-octadecyl-lauroylamide; OOGA, *N*-(β-D-glucopyranosyl)-*N*-octadecyl-oleoylamide; OSGA, *N*-(β-D-glucopyranosyl)-*N*-octadecyl-stearoylamide.

0006-3495/90/11/1199/08 $2.00

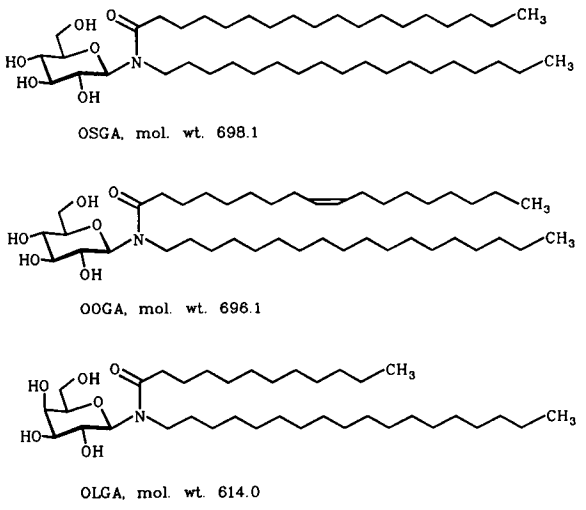

FIGURE 1 Structure formulae and molecular weights of the three glycolipids OSGA, OOGA, and OLGA.

with a slit collimated beam so that a desmearing of primary data was necessary. For this purpose an algorithm like the one described in reference 6 was used. The distance sample-detector is 20 cm, the detector can be moved over 30 mm in the direction perpendicular to the primary beam plane so that an angular range of 8.6° can be covered corresponding to a minimal Bragg distance of 10.3 Å with 1.542 Å radiation. Detector positioning and data registration were performed by a Z80-based microcomputer. For measurements at larger angles a Debye-Scherrer film camera was used.

For the x-ray measurements, the samples were sealed in quartz tubes of 1 mm diameter and 10 μm wall thickness. The tubes were inserted into a brass support, which can be heated electrically and cooled by evaporated liquid nitrogen. Electrical power and nitrogen flow were controlled by the microcomputer simulating a PID controller. A temperature stability of ±0.05K could be achieved in the range from −50 to 70°C.

Fig. 2 shows the diffraction patterns for a mixture of OOGA with 19.6 wt% water at three different temperatures. For the 50°C pattern, the raw data has been added (*dashed curve*) to demonstrate the effect of slit-length desmearing.

For the dielectric measurements a microwave bridge was constructed using X-band waveguide technique (7). The measuring frequency was set to 9.4 GHz. At this frequency the main dielectric effect is due to relaxation processes in water (the dielectric relaxation time of pure water at 0°C is $\tau_D = 0.11$ ns equivalent to a frequency of 9 GHz). The bridge was automatically balanced by a controller circuitry, which adjusted attenuator and phase shifter in the reference branch.

The samples were sealed in small rectangular teflon PFA containers and placed in the waveguide. Temperature control was performed by an arrangement similar to the one used in the x-ray measurements, but instead of a constant temperature, constant heating or cooling rates were programed (≈0.2 K/min).

The data were registered by a Professional 350 microcomputer (Digital Equipment Corp., Maynard, MA); it consisted of damping and phase shift due to the sample and its container as a function of temperature. From this data the complex dielectric function at the measuring frequency was calculated numerically (8, 9). This calculation was done in "real time" by the microcomputer while the measurement was running.

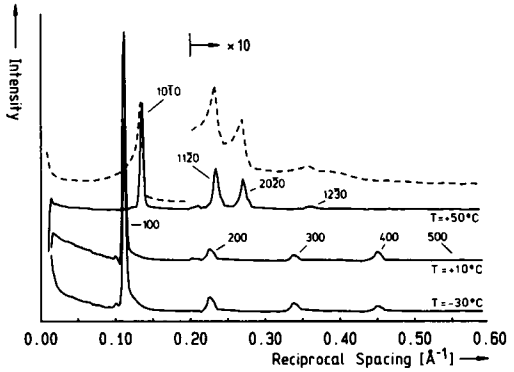

FIGURE 2 Sample diffractograms of OOGA with 19.6 wt% water at the temperatures −30, +10, and +50°C. The dashed curve represents raw data at $T = +50$°C. The solid curves show data after slit-length desmearing has been performed. To make the higher order reflections visible, the intensities have been multiplied by 10 in the range $k > 0.2$ Å.

The absolute value of the dielectric function determined by this procedure has an error <10%; the relative resolution, however, is much better than 1% assuming homogeneous samples. Sometimes the investigated samples get demixed during the experiment and in this way the dielectric response changes. The effective response of a heterostructure is always smaller than one would expect from the linear extrapolation of its components.

RESULTS

X-Ray measurements

Because the x-ray diffraction results are too extensive to be presented here in full length, only the data for the samples with highest water content are given for each glycolipid (Figs. 3–5). The diagrams show the distance *d* of the Bragg planes vs. temperature. In the case of

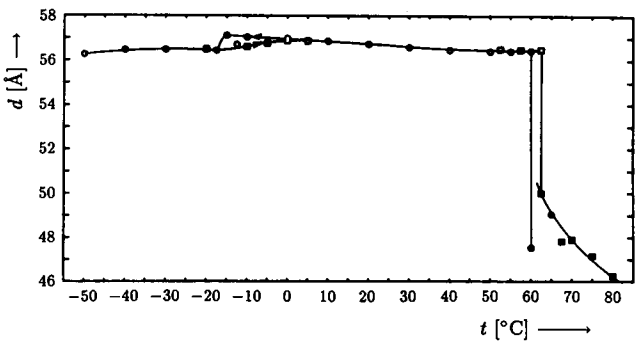

FIGURE 3 Bragg length *d* vs. temperature *t* in an OSGA/water sample with 29.7 wt% water content (*open symbols*, lamellar phase; *solid symbols*, hexagonal phase; *squares*, heating run; *circles*, cooling run; connected symbols indicate that two different Bragg lengths could be observed at the same temperature).

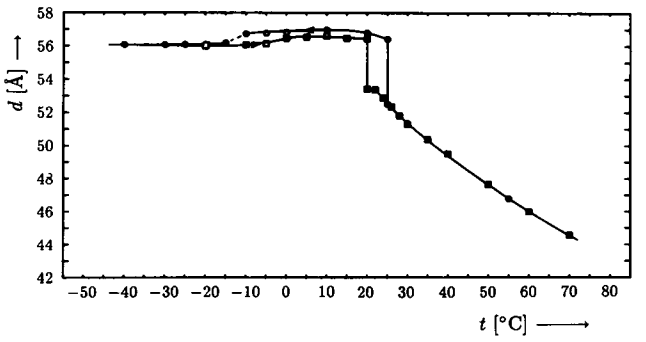

FIGURE 4 Bragg length d vs. temperature t in an OOGA/water sample with 29.7 wt% water content (symbols: cf. Fig. 3).

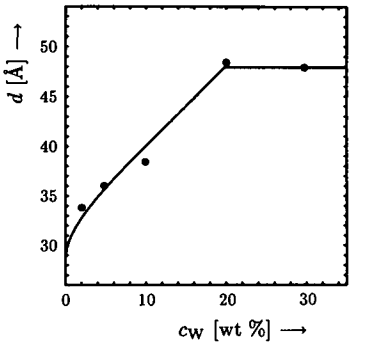

FIGURE 6 Bragg length d vs. water content c_W in OSGA/water samples at t = 70°C. The solid line displays the fit described in the Discussion section with the parameters d_{max} = 19.1 Å, saturation at 19.8 wt% water with d = 47.9 Å.

lamellar phases (*open symbols*), this value is the sum of lipid and water thicknesses, in the case of the hexagonal phase (*solid symbols*) it is $\sqrt{3}/2$ -times the distance of two unit cells or 3/2-times their lateral length. The appearance of the hexagonal structure can be identified clearly by a set of diffraction peaks with positions in the proportion $1:\sqrt{3}:2:\sqrt{7}:3\ldots$

For the diagrams concerning OSGA and OOGA two phase transitions can be observed: a well-pronounced lamellar ⟶ hexagonal transition at 20 and 60°C, respectively (henceforth called *main transition*), and a less remarkable one (lamellar ⟶ lamellar) at −15°C (*subzero transition*). The latter is observable by an −0.8 Å jump in d in the cooling run; when heating the sample, d restores its value continuously.

Comparison of the two diagrams shows that the introduction of a *cis*-double bond in one of the hydrocarbon chains has two effects: firstly, the main transition is shifted towards a lower temperature by ~40 K. Secondly, the values of the Bragg length d in the hexagonal phase are ≈3.5 Å larger at the same temperatures for the double bond containing OOGA.

The data of the third lipid species, OLGA, differs strongly from the other two: the subzero transition cannot be detected. An additional transition to a distorted hexagonal[2] structure is observed at 60°C, i.e., after the transition to the "normal" hexagonal structure at 45°C.

The corresponding results for lower water contents are not much different, except in the situation described below. In opposition to phospholipids the main transition temperature does not depend on water content c_W. The subzero transition can only be observed for OSGA with a minimum water content of 20 wt%, for OOGA with a minimum of 10 wt% water. Only the value of d in the hexagonal phase varies strongly (Figs. 6 and 7). The plots of d vs. c_W show that the hexagonal phase can hold up to ≈19 wt% water (the exact value depends on the lipid species and temperature) until it reaches saturation.

There is one exception to the general behavior found for OOGA with very low water contents: firstly, at 1.3 wt% the hexagonal phase can easily be supercooled to −40°C. The only effect of the main transition visible by x-ray diffraction is a minor increase (33.5 to 35 Å) of the Bragg length d of the hexagonal phase at 25°C and a partial conversion to the lamellar phase. It can be assumed that the hydrocarbon chains solidify in a glasslike state so that the hexagonal structure can be preserved. Total conversion to the lamellar phase can only be achieved if the

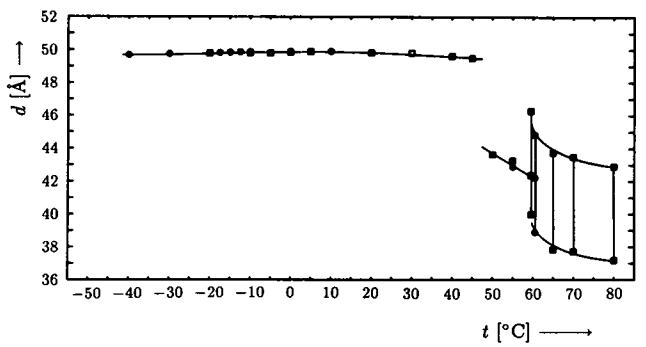

FIGURE 5 Bragg length d vs. temperature t in an OLGA/water sample with 19.8 wt% water content (symbols: cf. Fig. 3).

[2]The distorted hexagonal lattice is an oblique two-dimensional lattice in which the axes a, b, and the angle γ between them fulfill the relation $\cos\gamma = a/2b$. It can be derived from the (undistorted) hexagonal lattice by compressing or expanding it in the direction of one of its axes. It can be identified by the 110 peak in a position related to the 100 and 010 peak by $k^2_{110} = k^2_{100} + 2k^2_{010}$.

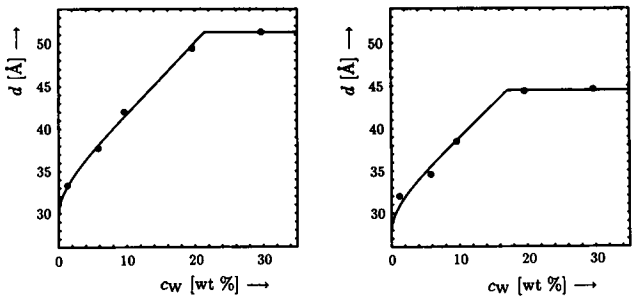

FIGURE 7 Bragg length d vs. water content c_W in OOGA/water samples at $t = 30°C$ (*left*) and $t = 70°C$ (*right*). The solid line displays the fit described in the Discussion with the parameters $d_{max} = 19.9$ Å and $d_{max} = 18.5$ Å resp., saturation at 21.4 wt% water with $d = 51.3$ Å and at 17.1 wt% water with $d = 44.4$ Å resp.

system is kept at temperatures closely below t_t (e.g., at 20°C) for a long time. The time constant for this conversion is 3 h (at 20°C). Secondly, this lamellar phase has an extremely low repeat distance in this system ($d = 51$ Å) and is much more disordered than in systems with higher water contents as can be seen from the width of the peaks. The first effect vanishes if the water content is raised to 6 wt%, so water acts as a lubricant for the structural transition $L_{\beta'} \rightarrow H_{II}$. The disordered lamellar phase can also be observed at 6 wt% water in coexistence with the normal lamellar phase, but not at 10 wt% water. Both effects cannot be found for OSGA, probably because its main transition temperature is much higher.

At selected t/c_W points, x-ray diffractograms were recorded with higher precision (registration time extended to 6 h, optimized angular positioning described in reference 10) to specify not only the spacing of the Bragg peaks but also their intensities. Due to the angular range limitation of the camera only the first five diffraction peaks could be recorded. With these results electron density profiles were constructed which show the laterally averaged electron density of the lamellar structures. A three-level step function model (hydrocarbon chains|headgroups|water) was fitted to the data to determine the phases. The results (step function and inverse Fourier transform of the phased intensities) for OOGA above and below the subzero transition are given in Fig. 8. The electron density profiles show that the water region diminishes from 5.6 to 2.7 Å due to this transition when cooling.

Dielectric measurements

Dielectric measurements were carried out only with OSGA and OOGA. Figs. 9 and 10 show the dependence of the complex dielectric function at 9.4 GHz on temperature for all investigated OSGA and OOGA samples. The

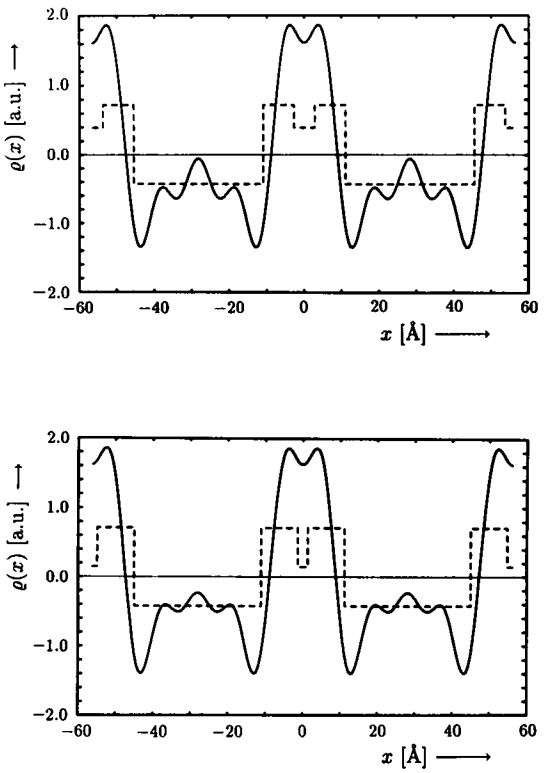

FIGURE 8 Electron density profiles (*solid lines*) and their step function models (*dashed lines*) of OOGA with 19.6 wt% water above the subzero transition ($t = +10°C$, upper diagram) and below ($t = -30°C$, lower diagram). The electron density is given in arbitrary units as the difference to the average electron density.

values for ϵ_1 and ϵ_2 increase monotonically with the water content due to its high polarizability.

The plot of Fig. 9 shows that the main transition causes a negative step in both parts of the dielectric function, which becomes more pronounced as more water is added. The overall feature of the dielectric response is that for a water content up to 15 wt% both ϵ_1 and ϵ_2 increase with T. According to the Debye model this means that the measuring frequency is larger than the relaxation frequency of the bound water. However, the sample having 30 wt% water displays an increasing ϵ_1 and a decreasing ϵ_2 as a function of temperature. This behavior indicates that now the effective dielectric function is governed by a relaxation frequency higher than the measuring frequency. The relaxation frequency is in this case approaching that of pure water, which is 17 GHz at room temperature.

The OOGA samples show small peaks in ϵ_2 near 45°C, particularly at 7 wt% (Fig. 10). The absorption signals are not accompanied by a significant phase shift (ϵ_1). We don't have an interpretation for those peaks for the time being.

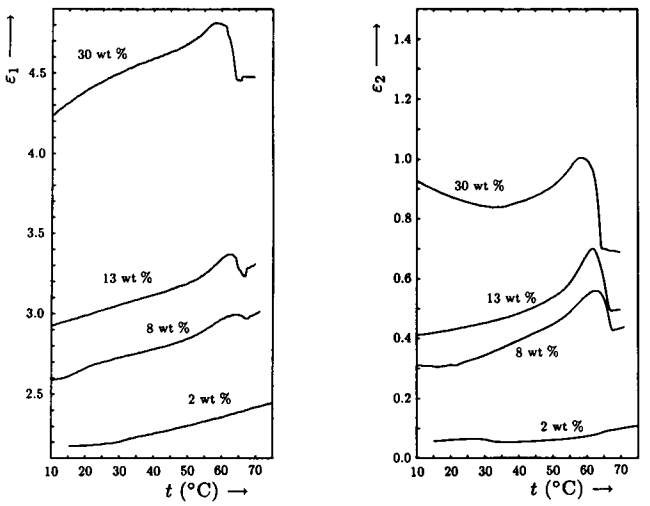

FIGURE 9 Real part (ϵ_1, left) and imaginary part (ϵ_2, right) of the dielectric function at 9.4 GHz for four OSGA samples with different water contents given by the values adjacent to the curves (heating rate: 0.2 K/min).

The dielectric response reveals a temperature shift of the phase transition of OSGA (Fig. 9) between 8 and 30 wt%. This result is in qualitative agreement with the behavior of phospholipid bilayers, where the transition temperature increases with decreasing water concentration too, but the amount of the shift is much smaller in the present case.

Fig. 11 shows an example for the dielectric behavior of the glycolipid/water mixtures below 0°C (OOGA with 15 wt% water). In the cooling run ϵ_1 and ϵ_2 abruptly drop down to nearly the value of dry OOGA (2.2 + 0.05i) at $t_f = -16$°C, which is the same temperature where the jump in d occurs in the x-ray measurements. Upon heating the original value of ϵ is restored at $t_m \lesssim 0$°C apart from a small overshoot. This behavior is likewise observed for all OSGA samples with $c_W \geq 13$ wt% and for OOGA with $c_W \geq 7$ wt%.

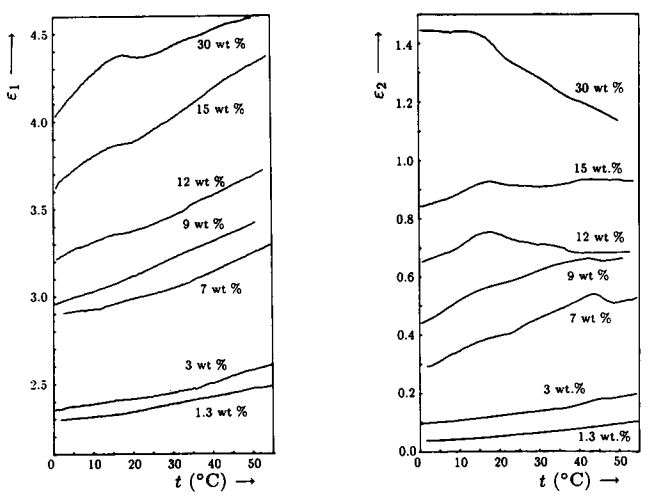

FIGURE 10 Real part (ϵ_1, *left*) and imaginary part (ϵ_2, *right*) of the dielectric function at 9.4 GHz for seven OOGA samples with different water contents given by the values adjacent to the curves (heating rate, 0.2 K/min).

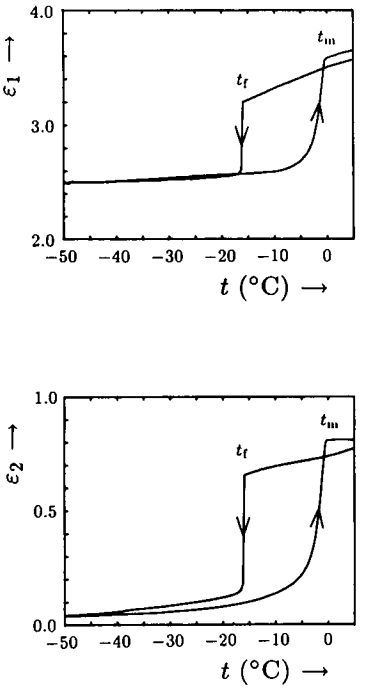

FIGURE 11 Real part (ϵ_1, upper) and imaginary part (ϵ_2, lower) of the dielectric function at 9.4 GHz of OOGA with 15 wt% water at temperatures <0°C (cooling rate, 0.2 K/min; heating rate, 0.1 K/min).

DISCUSSION

The main question concerning the hexagonal phase is whether its structure is H_I or H_{II} (Fig. 12). Both possibilities cannot be discriminated solely upon the diffraction

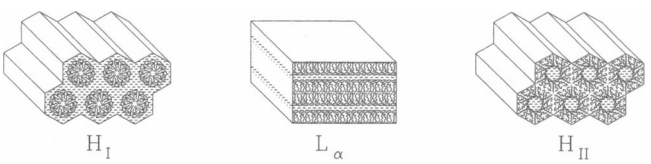

FIGURE 12 H_I, L_α, and H_{II} structure of lipid/water phases.

patterns because a region of higher electron density embedded in a bulk with smaller electron density yields the same diffraction like the opposite arrangement (this is a consequence of Babinet's principle).

Evidence that in our case the hexagonal phase is of type H_{II} can be derived from a calculation of the area per lipid headgroup for low water content. A value of 33.4 Å^2 is obtained assuming the H_{II} structure for OOGA with 9.6 wt% water at t = 60°C. Under the H_I hypothesis the calculation yields 114 Å^2 (the calculation is described to full extent in reference 10 and is a slight modification of the one described in reference 11). The second value can be ruled out because one molecule of glucose is unable to cover this area so that an H_I structure would cause a contact of hydrophobic chains with water. This result is in accordance with x-ray investigations on mono- and diglycosyldiacylglycerols which show that the MGDGs form H_{II} phases but the DGDGs form lamellar phases (2).

For the lamellar structure there are several variants possible *a priori* too. Firstly, the question arises whether the hydrocarbon chains are in a molten state (L_α) or in a rigid all-*trans* conformation (L_β or $L_{\beta'}$). In all cases the large angle x-ray diffraction yielded sharp peaks for the lamellar phases indicating that the chains are laterally ordered, which is only possible in the all-*trans* state. Secondly, the chains can be oriented either perpendicular to the lamella plane (L_β) or tilted ($L_{\beta'}$). A comparison of the lipid thickness determined from electron density profiles or calculated from the area per lipid molecule and the molecule's volume results in a tilt angle of 23–34° for OSGA, 24–29° for OOGA, and 19° for OLGA (Table 1). So all lipids are in the $L_{\beta'}$ state.

The fact that the repeat distance does not show any discontinuity below the main transition proves that there is no intermediate L_α phase (as e.g., in the case of DAPE [12]): chain melting and reordering of the structure happen at the same temperature t_t (direct transition).[3]

TABLE 1 Separation of the Bragg length d into lipid and water layer thicknesses d_L and d_W resp. and resulting tilt angle (using a molecule length of 29 Å for OSGA and OOGA, 25 Å for OLGA)

Lipid	Water	t	d	d_L	d_W	Method
	wt %	*°C*	Å	Å	Å	
OSGA	2.0	+23	55.2	52.7	2.5	25° LA
OSGA	4.8	+23	55.7	48.3	7.4	34° LA
OSGA	9.9	+23	56.7	53.2	3.5	23 LA
OSGA	20.0	+23	57.2	52.9	4.3	24° LA
OOGA	9.6	+10	56.3	51.9	4.4	27° ED
OOGA	9.6	−30	55.8	52.9	2.9	24° ED
OOGA	19.6	+10	56.5	50.9	5.6	29° ED
OOGA	19.6	−30	56.2	53.5	2.7	23° ED
OLGA	19.8	+10	49.7	47.2	2.5	19° ED
OLGA	19.8	−30	49.8	47.3	2.5	19° ED

The methods applied were ED, from the step function model for the electron density; and LA, the bilayer area per lipid molecule was determined from large angle x-ray diffraction. From this value and a volume of 1,160 Å^3 per molecule the bilayer thickness was calculated.

The main transition has a mediate effect on the dielectric data: the drop in both parts of the dielectric function, which occurs only in the presence of sufficient water, shows that the spectrum of bound water relaxation is shifted towards lower Debye frequencies in this transition, giving lower contributions to the dielectric function at the measuring frequency (13). So, more water can be bound in the hexagonal phase and/or water is bound tighter, thus, reducing its dielectric response. The same behavior was observed in DMPC/water systems (4, 14), but in the latter systems also, the direct dielectric effect of chain melting was found.

Our interpretation is based on the decreasing ratio $\Delta\epsilon_1/\Delta\epsilon_2$ with decreasing water content at the transition, which is in qualitative agreement with the Debye relaxator model. The interpretation is also compatible with a decrease of polarizable water molecules at the measuring frequency due to more strongly localized water molecules above the phase transition. For instance, in ice the Debye frequency is lowered by about three orders of magnitude compared to liquid water.

The subzero transition, which is connected with the hysteresis in $d(t)$ and $\epsilon(t)$, has already been found in phospholipid (16) and glycolipid systems (17). It can be explained as freezing of supercooled water: because the interlamellar water is in contact only with the smooth surfaces of the lipid bilayers it can be cooled down to t_f = −16°C until freezing starts. Then a separate ice phase is formed which can absorb water from the lipid/water phase until the chemical potential of water in both phases equalizes.[4] This causes the reduction of 0.8 Å of the repeat length at t_f. As can be seen from the electron density profiles, the effect would be even larger if the reduction of the water layer were not partially compensated by an expansion of the lipid bilayer. A similar compensation could be found in the DMPC/water system

[3]Chain melting is a necessary condition for rearranging the lipid molecules in a way that they can form a hexagonal phase, so it always occurs at a lower or equal temperature than the transition $L_{\beta'} \rightarrow H_{II}$. (Of course, a glassy state would also be possible, but this also requires previous melting.) On the other hand chain melting would cause a reduction of the repeat distance d in an L → L transition because the effective length of the hydrocarbon chains diminishes due to the occurrence of gauche-bonds, a behavior which is not observed here.

[4]Removing water from the lamellar phase reduces the water layer thickness d_W. This in turn intensifies the hydration force (15) repelling the bilayers. This force can in another way be viewed as an extra term in the chemical potential keeping the water in the lipid/water phase.

(18), but in the latter case a net effect remains which is much greater (≈10 Å). In the microwave measurements, freezing of the water causes the dielectric function to drop because the dielectric response of ice is much smaller in the microwave region due to its essentially lower Debye frequency.

When the system is heated up again the water returns from the ice phase to the lipid/water phase always maintaining the equality of chemical potentials. So the variables $d(t)$ and $\epsilon(t)$, which depend on the amount of (liquid) water, continuously restore their previous values at t_m. The fact that in most measurements an overshoot in ϵ can be observed, whereas d does remain some tenth of an angstrom lower than the value of the cooling run, can be explained by a little amount of water which remains outside the lamellar phase at $t \geq t_m$ because the speed of absorption into this phase is very low when the difference in chemical potentials becomes small.

As mentioned, the effect of the subzero transition is small in comparison to its effect in phospholipid/water systems. Despite that this can be attributed by part to the compensation effect, it still remains remarkable. Together with the weak dependence of the main transition temperature t_t on water content this suggests that the lipid/water interaction is much weaker in the glycolipids investigated here. This can be related to the fact that the headgroup is fixed much more rigidly by the *N*-bonding than it is in natural lipids with a flexible glycerol backbone. This rigidity may hinder the hydration of the headgroup sterically.

This is also supported by the dielectric data: the maximum of the imaginary part of the dielectric functions is found for OSGA and OOGA with 30 wt% water at −1°C. The corresponding value for pure water is −1.5°C, for DPPC (a phospholipid) with 29 wt% water at +8°C (19). The maximum of ϵ_2 vs. temperature indicates the identity of the water Debye frequency and the measuring frequency. Thus, the experimental results show that at the same temperature pure water has a higher relaxation frequency than water in the hydrophilic surroundings of the glycolipids and a fortiori in those of the phospholipids. This shift can be considered as an integral measure for the strength of binding between water and lipid headgroups. It indicates that water is much less influenced in the present systems.

The maximum of hydration of the $L_{\beta'}$ phase could not be determined in the usual way by plotting the repeat distance d of the lamellar structure vs. water concentration c_W (as, e.g., in reference 20) and looking for the concentration where no further swelling takes place. Considering the experimental errors, d showed no variation at all when water was added. However it is possible to calculate the water content of the lamellar phase from the data of Table 1 which includes the thickness of the water layer d_L. (d_L/d) is the volume fraction of water incorporated in the lamellar phase. In all but one case this value is <10%.

In contrast to this the Bragg length in the H_{II} phase shows a clear dependence $d(c_W)$. Interestingly, when the structural parameters of this phase were calculated the parameter d_{max} (Fig. 13) turned out to be nearly constant. This parameter, whose importance for H_{II} phases Seddon et al. already pointed out (21), gives the maximum distance of the water region from the border of the hexagonal unit cell, i.e., the maximum elongation of a lipid molecule. The data fit well with d_{max} = constant implying that

$$d(c_W) = \frac{3}{2} d_{max} \Big/ \left(1 - \sqrt{\frac{3\sqrt{3}}{2\pi} \frac{c_W \bar{v}_W}{(1 - c_W)\bar{v}_W + C_W \bar{v}_W}}\right)$$

where $\bar{v}_L \approx \bar{v}_W = 1\ cm^3/g$ are the specific volumes of lipid and water. Concerning the quality of the fits it has to be taken into account that the water content for the x-ray measurement samples could not be specified with more accuracy than 1 wt%.

The maximum elongation d_{max} seems to be the limiting factor for the structure of the H_{II} phase. As can be seen from the data for OOGA this value shrinks with rising temperature because the introduction of additional gauche conformations effectively shortens the hydrocarbon chains. Comparison with OSGA at 70°C shows that d_{max} is

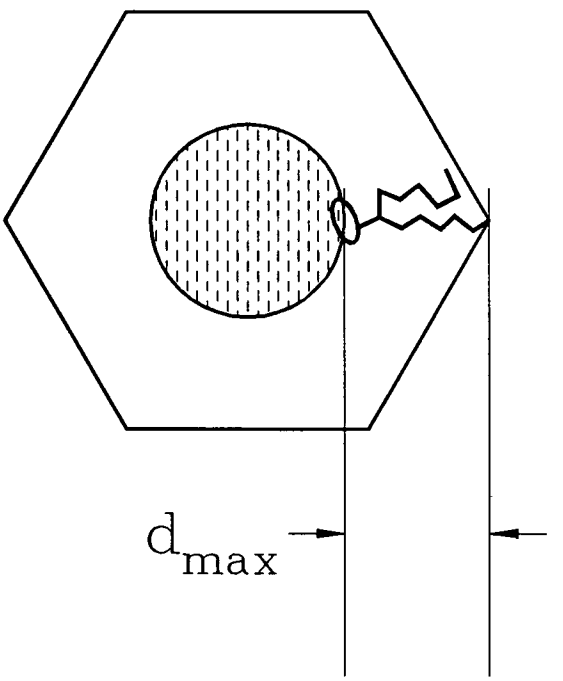

FIGURE 13 Structural parameter d_{max}, maximum elongation of a lipid molecule in the H_{II} phase.

smaller for OOGA with its double bond. Obviously it acts as a "permanent kink" in addition to those generated by thermal excitation.

Surprisingly, the double bond in the chain region also affects the limit hydration of the H_{II} phase which on the first guess should only depend on the headgroup region, which is identical for both lipids. For OSGA, saturation is reached at 20 wt%, for OOGA at 17 wt%. This extra water bound by OSGA remains bound even in the subzero phase according to calculations of Grünert (8). In this phase OSGA still contains 4–6 molecules of water per lipid molecule (equivalent to 9–13 wt%), whereas OOGA holds 1–3 (2–7 wt%) only. So it seems that the double bond has an influence which extends up to the lipid/water interface perhaps changing the arrangement of headgroup sugar molecules.

As already mentioned, OLGA shows greater differences to the other two glycolipids. First of all, the distorted hexagonal phase appears. This may be a consequence of the asymmetric hydrocarbon chains orienting themselves in a way that the longer octadecyl chains assemble in the perpendicular direction to the shorter laureoyl chains. Another difference is that OLGA shows no subzero transition. In accordance with the electron density profile this indicates that OLGA is only very little hydrated ($\approx$4 wt%) in the $L_{\beta'}$ phase. Whether this is a consequence of the headgroup region or the hydrocarbon chains cannot be discriminated because both are different from those in OSGA and OOGA.

We wish to thank A. Kops for his help in constructing the x-ray sample holder and Dr. A. Enders for valuable discussions and critical proofreading of the manuscript.

We thank the Ministerium für Wissenschaft und Forschung des Landes Nordrhein-Westfalen for financial support of the research project.

Received for publication 4 April 1990 and in final form 20 June 1990.

REFERENCES

1. Hakomori, S. 1981. Glycosphingolipids in cellular interaction, differentiation, and oncogenesis. *Annu. Rev. Biochem.* 50:733–764.
2. Curatolo, W. 1986. The physical properties of glycolipids. Biochim. Biophys. Acta. 906:111–136.
3. Stünkel, K. G., O. Lockhoff, H. G. Opitz, V. Klimetzek, G. Streissle, A. Paessens, P. Stadler, and H. D. Schlumberger. 1988. Synthetic glycolipids: in vitro characterization of a new class of compounds with immunomodulating properties. *Adv. Biosci.* 68:429–437.
4. Enders, A., and G. Nimtz. 1984. Dielectric relaxation study of dynamic properties of hydrated phospholipid bilayers. *Ber. Bunsen-Ges. Phys. Chem.* 88:512–517.
5. Nimtz, G., B. Binggeli, L. Börngen, P. Marquardt, U. Schäfer, and R. Zorn. 1986. Dielectric and structural properties of a water–oil emulsion at the gel-microemulsion transition. *Europhys. Lett.* 2:103–108.
6. Akiyama, M. 1981. Slow change in the repeat period of multilamellar dimyristoylphosphatidylcholine accompanied by thermal phase transition. *Biochim. Biophys. Acta.* 644:89–95.
7. Grünert, M. 1988. Dielektrische Mikrowellenmessungen zur Charakterisierung der Flüssigkristallinen Phasen und der Eigenschaften des Wassers in Lipid/Wasser-Systemen. Ph.D. thesis. Universität zu Köln, Köln, FRG.
8. Enders, A. 1989. An accurate measurement technique for line properties, junction effects, and dielectric and magnetic material parameters. *IEEE (Inst. Electr. Electron. Eng.) Trans. on Microwave Theory and Techniques.* 37:598–605.
9. Enders, A. 1989. Dynamische Eigenschaften von Anästhetikadotierten Modellmembranen bei Mikrowellenfrequenzen. Ph.D. thesis. Universität zu Köln, Köln, FRG.
10. Zorn, R. 1989. Röntgenbeugungsmessungen an Flüssigkristallinen Glykolipid/Wasser-Systemen. Ph.D. thesis. Universität zu Köln, Köln, FRG.
11. Luzzati, V. 1968. X-Ray diffraction studies of lipid-water systems. *In* Biological Membranes. D. Chapman, editor. Academic Press Limited (AP), London.
12. Seddon, J. M., G. Cevc, R. D. Kaye, and D. Marsh. 1984. X-Ray diffraction study of the polymorphism of hydrated diacyl- and dialkylphosphatidylethanolamines. *Biochemistry.* 23:2634–2644.
13. Nimtz, G. 1986. Magic numbers of water molecules bound between lipid bilayers. *Physica Scripta.* T13:172–177.
14. Enders, A., and G. Nimtz. 1985. Correlation and dynamics of acyl-chain isomerization rotation in dimyristoylphosphatidylcholine bilayers. *Phys. Rev. A.* 32:2521–2523.
15. Parsegian, V. A., N. Fuller, and R. P. Rand. 1979. Measured work of deformation and repulsion of lecithin bilayers. *Proc. Natl. Acad. Sci. USA.* 76:1750–1754.
16. Grünert, M., L. Börngen, and G. Nimtz. 1984. Structural phase transition due to a release of bound water in phospholipid bilayers at temperatures below 0°C. *Ber. Bunsen-Ges. Phys. Chem.* 88:608–612.
17. Grünert, M. 1984. Physikalische Eigenschaften des Flüssigkristallinen Systems Digalaktosyldiazylglyzerid/Wasser. Masters thesis. Universität zu Köln, Köln, FRG.
18. Zorn, R. 1985. Röntgenbeugungsuntersuchungen an Flssigkristallinen Systemen. Masters thesis. Universität zu Köln, Köln, FRG.
19. Börngen, L. 1985. Dynamische und Strukturelle Eigenschaften der Modellmembransysteme DMPC/Wasser, DPPC/Wasser und DSPC/Wasser. Ph.D. thesis. Universität zu Köln, Köln, FRG.
20. Janiak, J., M. Small, and G. Shipley. 1979. Temperature and compositional dependence of the structure of hydrated dimyristoyl lecithin. *J. Biol. Chem.* 254:6068–6078.
21. Seddon, J. M., G. Cevc, and D. Marsh. 1983. Calorimetric studies of the gel-fluid ($L_\beta - L_\alpha$) and lamellar-inverted hexagonal ($L_\alpha - H_{II}$) phase transitions in dialkyl- and diacylphosphatidylethanolamines. *Biochemistry.* 22:1280–1289.